Archives of Biochemistry and Biophysics 608 (2016) 20–26

Contents lists available at ScienceDirect

Archives of Biochemistry and Biophysics

journal homepage: www.elsevier.com/locate/yabbi

Biochemical and structural characterization of quinoprotein aldose sugar dehydrogenase from *Thermus thermophilus* HJ6: Mutational analysis of Tyr156 in the substrate-binding site

Han-Woo Kim [a, b], Ji-Yeon Wang [c], Ji-Yeon Lee [c], Ae-Kyung Park [a], Hyun Park [a, b], Sung-Jong Jeon [c, d, *]

[a] Division of Life Sciences, Korea Polar Research Institute (KOPRI), Korea University of Science and Technology, 26 Songdomirae-ro, Incheon, 21990, Republic of Korea
[b] Department of Polar Sciences, Korea University of Science and Technology, 26 Songdomirae-ro, Incheon, 21990, Republic of Korea
[c] Department of Biotechnology & Bioengineering, Dong-Eui University, 176 Eomgwangno, Busanjin-gu, Busan, 47340, Republic of Korea
[d] Department of Smart-Biohealth, Dong-Eui University, 176 Eomgwangno, Busanjin-gu, Busan, 47340, Republic of Korea

ARTICLE INFO

Article history:
Received 17 June 2016
Received in revised form
18 August 2016
Accepted 30 August 2016
Available online 31 August 2016

Keywords:
Thermus thermophilus
Aldose sugar dehydrogenase
Soluble quinoprotein glucose dehydrogenase
Alcohol oxidation

ABSTRACT

The gene encoding a quinoprotein aldose sugar dehydrogenase (ASD) from *Thermus thermophilus* HJ6 (Tt_ASD) was cloned and sequenced; it comprised 1059 nucleotides encoding a protein containing 352 amino acids that had a predicted molecular mass of 38.9 kDa. The deduced amino acid sequence showed 42.9% and 33.9% identities to the ASD proteins from *Pyrobaculum aerophilum* and *Escherichia coli*, respectively. The biochemical properties of Tt_ASD were characterized. The optimum pH for the oxidation of glucose was 7.0–7.5 and the optimum temperature was 70 °C. The half-life of heat inactivation for the apoenzyme was about 25 min at 85 °C. The enzyme was highly thermostable, and the activity of the pyrroloquinoline quinone-bound holoenzyme was not lost after incubation at 85 °C for 100 min. Tt_ASD could oxidize various sugars, including hexoses, pentoses, disaccharides, and polysaccharides, in addition to alcohols. Structural analysis suggested that Tyr156 would be the substrate-binding residue. Two mutants, Y156A and Y156K, had impaired activities and affinities for all substrates and completely lost their activities for alcohols. This structural and mutational analysis of Tt_ASD demonstrates the crucial role of Tyr156 in determining substrate specificity.

1. Introduction

PQQ-dependent dehydrogenases are the largest enzyme group within the quinoprotein family [1]. PQQ is synthesized exogenously and then associates with an apoprotein to form the active holoenzyme. The PQQ enzymes are broadly classified as quinoprotein alcohol dehydrogenases (ADH) and quinoprotein glucose dehydrogenases (GDH). Quinoprotein ADH, which catalyzes the oxidation of alcohols into the corresponding aldehydes, is classified into three types. Type I comprises methanol dehydrogenase (MDH) and ethanol dehydrogenase. Type II ADH is a soluble quinohemoprotein having a C-terminal extension containing heme C. Type III ADH, a membrane-bound quinohemoprotein, is found only in acetic acid bacteria [2,3]. Quinoprotein GDH catalyzes the oxidation of glucose and other aldoses to their corresponding aldono-δ-lactones with concomitant reduction of its cofactor, PQQ. Two kinds of PQQ-GDHs are known; one is a soluble glucose dehydrogenase (sGDH) that has only been found in the periplasm of *Acinetobacter calcoaceticus* [4] and the other is a membrane-bound form (mGDH) that is widespread in gram-negative bacteria. Of these, mGDH has high glucose selectivity but requires suitable detergents for solubilization and purification [5], while sGDH exhibits low substrate specificity and lacks thermal stability [6,7].

A. calcoaceticus sGDH (Ac_sGDH), which has been extensively characterized and structurally defined, has a β-propeller fold comprising six four-stranded, antiparallel β-sheets [8]. This enzyme is homodimeric, consisting of identical subunits of 50 kDa, and contains one PQQ per subunit. Ca^{2+} has a dual role in sGDH, being

Abbreviations: Ac, *Acinetobacter calcoaceticus*; ASD, aldose sugar dehydrogenase; Ec, *Escherichia coli*; Pa, *Pyrobaculum aerophilum*; PQQ, pyrroloquinoline quinone; sGDH, soluble glucose dehydrogenase; ADH, alcohol dehydrogenase; MDH, methanol dehydrogenase; Tt, *Thermus thermophilus*.

* Corresponding author. Department of Biotechnology and Bioengineering, Dong-Eui University, 176 Eomgwangno, Busanjin-gu, Busan, 47340, Republic of Korea.
E-mail address: jeon.sj@deu.ac.kr (S.-J. Jeon).

http://dx.doi.org/10.1016/j.abb.2016.08.022
0003-9861/

required for dimerization and for binding of PQQ [9]. The enzyme oxidizes a wide variety of pentose and hexose sugars, both mono- and di-saccharides, into their corresponding lactones [10]. sGDH is able to donate electrons to several neutral or cationic artificial electron acceptors, including *N*-methylphenazonium methyl sulfate [11] and electroconducting polymers [12]. The enzyme has a high turnover number and electrochemical regeneration of the PQQ cofactor can be easily achieved without negative effects of O_2 tension and product inhibition. Therefore, sGDH has been utilized for glucose-based biosensors [9] and biofuel cells [13–15].

Recently, a novel soluble quinoprotein sugar dehydrogenase (Ec_ASD) was identified in *Escherichia coli* [16]. The amino acid sequence of Ec_ASD shows a relatively low identity (18%) with Ac_sGDH, and the native state of enzyme is a monomer, whereas that of Ac_sGDH is a dimer. In addition, this enzyme has a low affinity for both glucose and maltose, but converts a wide range of mono-, di-, and tri-saccharide aldose sugars into their corresponding lactones. The crystal structure of Ec_ASD revealed major structural differences in the loop and surface-exposed regions, compared with Ac_sGDH, although the β-propeller fold is conserved [16]. Based on catalytic and structural differences between Ac_sGDH and Ec_ASD, it has been proposed that Ec_ASD represents a new subgroup of PQQ-dependent soluble dehydrogenases that is distinguishable from Ac_sGDH and has been named the soluble aldose sugar dehydrogenase (ASD) group [16]. In Archaea, an ASD from *Pyrobaculum aerophilum* (Pa_ASD) has been identified and structurally defined. Catalytic and structural analysis of this protein showed that it has significant similarity to Ec_ASD [17].

In the genome databases of the thermophilic bacterium *Thermus thermophilus* strains HB8, HB27, JL-18, and SG0.5JP17-16, we found putative homologues of the sGDH gene. *T. thermophilus* HJ6 is an aerobic chemoorganotroph, gram-negative, rod-shaped, and extremely thermophilic bacterium that grows between 80 and 95 °C and optimally at 80 °C [18]. In this study, we cloned and expressed the gene encoding a sGDH homolog from *T. thermophilus* HJ6 in *E. coli*. We describe the structural analysis and biochemical characterization of the recombinant protein and also report a mutational analysis of the residue Tyr156 located in the substrate-binding site.

2. Materials and methods

2.1. Chemicals, strains, and plasmids

DNA primers and substrates were prepared by Bioneer (Daejeon, Korea). Taq DNA polymerase was purchased from Takara (Tokyo). Chemicals used for the determination of laccase activity were obtained from Sigma Chemical Co. (St. Louis, MO, USA). All other chemicals used were of reagent grade. *E. coli* DH5α and BL21 Codon-Plus (DE3) (Novagen, Inc., San Diego, CA, USA) were used as the cloning and expression host cells, respectively. The plasmid pET-21a was purchased from Novagen as the expression vector for the enzyme protein.

2.2. Cloning and DNA sequencing

Chromosomal DNA of *T. thermophilus HJ6* was prepared using the GeneAll® GENEx Genomic kit (GeneAll Biotechnology, Seoul, Korea). To obtain the ASD gene from HJ6, PCR was performed using two primers (F1, 5′-GTCGGGGAAGGGGGTGGCTG-3′ and R1, 5′-AGGTCCGCTTCCGCAAGAGG-3′) which were designed based on the upstream sequence of the initiation codon (GTG) and the downstream sequence of the termination codon (TAG), for sGDH gene from the genome sequence of *T. thermophilus* HB8, HB27, or JL-18. DNA amplification was carried out using Taq DNA polymerase for 30 cycles at 95 °C for 30 s, 55 °C for 60 s, and 72 °C for 60 s. To prepare templates for sequencing, the amplified 1.11-kbp fragment was cloned into pGEM®-T as an asd candidate and the construct was designated as pGEM-asd. DNA sequencing analysis was performed by an ABI Prism 3700 genetic analyzer (Perkin–Elmer Applied Biosystems, Foster City, CA, USA).

2.3. Construction of the wild-type and mutant enzymes

The gene was amplified by PCR using the pGEM-asd plasmid DNA as a template, and two primers: F2, 5′-GGGGTGGCATATGGACCGGAGGCGCTTTCT-3′ (the *Nde* I site is underlined); and R2, 5′-CCGAAGCTTAAGGAGGCGTAGCACCCGG-3′ (the *Hin*d III site is underlined). PCR amplification was conducted for 30 cycles at 94 °C for 30 s, 60 °C for 30 s, and 74 °C for 1 min for 30 cycles using Pfu DNA polymerase (INTRON Biotech., Korea). An amplified 1.07-kbp DNA fragment was digested with the restriction enzymes *Nde* I and *Hin*d III, and inserted into the pET-21a that contains a region coding for His-tag sequence. The resulting plasmid was designated as pET-asd.

The Y156A mutant construct was generated by introducing a point mutation into the wild-type ASD vector, pET-asd using a site-directed mutagenesis kit (Muta-DirectTM, iNtRon). The primers were F3: 5′-GGGGAGGTCGCCGAGCGGGAG-3′, R3: 5′-CTCCCGCTCGGCGACCTCCCC-3′. The Y156K mutation was then introduced into pET-asd using the same technique. The primers were F4: 5′-GGGGAGGTCAAAGAGCGGGAG-3′, R4: 5′-CTCCCGCTCTTTGACCTCCCC-3′. The mutated nucleotides are underlined. All mutations were verified by nucleotide sequencing.

2.4. Expression and purification of His-tagged ASD and mutants

His-tagged ASD and mutants were expressed independently as follows. *E. coli* BL21 Codon-Plus (DE3) cells harboring constructed pET-asd plasmid to an OD_{600} of approximately 0.5 and then inducing expression with 0.3 mM IPTG for 16 h at 25 °C. The cells were centrifuged and the pellet was washed with resuspension buffer (50 mM Tris-HCl, pH 7.5, 500 mM NaCl). The cells were then disrupted by sonication and supernatant fraction was recovered by centrifugation at 27,000×*g* for 30 min. The supernatant fraction was heat-treated at 75 °C for 20 min followed by recentrifugation. The supernatant was applied to HisTrap HP column (GE Healthcare) and washed with at least 10 column volumes (CV) of the resuspension buffer, and the ASD-His_6 fusion protein was finally eluted at a flow rate of 1 ml/min with a linear gradient of 0–500 mM imidazole in resuspension buffer using ÄKTAprime (GE Healthcare). The purity of the fusion protein was confirmed by SDS-PAGE. Protein concentration was determined using a Bio-Rad protein assay system (Bio-Rad, Hercules, CA, USA) with bovine serum albumin as the standard.

2.5. Enzyme reconstitution with PQQ

Reconstitution of the apoenzyme with PQQ was carried out using a method similar to that described by Southall et al. [16]. The purified protein (1.7 mg/ml) was incubated for 16 h min at 25 °C with a 10-fold molar excess of PQQ in buffer containing 20 mM Tris-HCl (pH 7.5), 100 mM NaCl and 1 mM $CaCl_2$. Unbound PQQ was removed by passing the mixture over a Sephadex G-25 column (PD-10; GE Healthcare).

2.6. Enzyme assay and kinetic calculations

Enzyme activity was determined spectrophotometrically at 70 °C by following the reduction of 2,6-dichlorophenol-indophenol

(DCIP) at 600 nm, using phenazine methosulfate (PMS) as a primary electron acceptor. The standard reaction mixture contained 50 mM Tris-HCl (pH 7.5), 100 mM D-glucose, 0.06 mM DCIP ($\varepsilon_{600} = 21.0\ mM^{-1}\ cm^{-1}$); 0.6 mM PMS and the enzyme (10 μg) in a total volume of 1 ml. To determine the activity of the apoenzyme, 1 μM PQQ was added to the reaction mixture. The initial decrease in the absorbance at 600 nm was measured continuously with a spectrophotometer (Optizen 2120UV, Mecasys, Korea) equipped with a thermostat. One unit of enzyme activity was defined as the reaction of 1 μM of sugar substrate per minute. To evaluate substrate specificity, D-glucose in the standard reaction mixture was replaced by several sugars and alcohols. For the kinetic analyses, various concentrations of D-glucose (0.01–0.8 M), D-galactose (0.01–0.8 M), D-mannose (0.01–1.2 M), L-arabinose (0.01–0.8 M), D-xylose (0.01–1.2 M), D-ribose (0.01–0.5 M), 2-deoxy-glucose (0.05–0.8 M), glucosamine (0.01–0.3 M), glucose 6-phosphate (0.01–0.3 M), maltose (0.01–0.8 M), α-Lactose (0.01–0.5 M), D-cellobiose (0.01–0.4 M), maltotriose (0.01–0.5 M), xylitol (0.02–0.5 M), mannitol (0.1–0.7 M), methanol (0.05–0.5 M), and ethanol (0.05–0.5 M) were used. The K_m value was determined measuring the initial velocity, and the apparent k_{cat} was determined from k_{cat} $t = V_{max}$/[enzyme]. All kinetic studies were performed at least twice and the kinetic data was calculated according to the procedure of Michaelis-Menten equation by EZ-Fit program [19].

2.7. Temperature and pH optimum

The temperature dependence of the activity was determined in 50 mM Tris-HCl (pH 7.5) using glucose as a substrate. To determine the optimum temperature for ASD activity, its activity was measured at temperatures ranging from 30 to 90 °C. The optimum pH for its reaction was estimated by monitoring activity at pHs of 5.0–9.5 using the following buffers: 50 mM sodium acetate buffer for pH 5.0–6.0; 50 mM sodium phosphate buffer for pH 6.0–7.5; 50 mM Tris–HCl buffer for pH 7.5–8.5; 50 mM glycine-NaOH for pH 8.5–9.5. The thermostability of the apo- and holoenzymes was determined by incubating them (1.0 mg/ml in 50 m M Tris-HCl buffer, pH 7.5) for various lengths of time at 85 °C and then detecting the remaining activity by running the standard assay at 70 °C.

3. Results and discussion

3.1. Identification of asd

The PCR product for the entire open reading frame (ORF) of a putative *asd* was amplified from the chromosomal DNA of *T. thermophilus* HJ6, cloned into the pGEM-T vector, and sequenced (for detail see "Materials and methods"). The ORF encoded a protein comprising 352 amino acids with a predicted molecular weight of 38.9 kDa and an estimated isoelectric point of 10.17. Fig. 1 shows schematic drawings of the alignment of a putative ASD from *T. thermophilus* HJ6 with its homolog. The deduced amino acid sequence of a putative ASD from *T. thermophilus* HJ6 showed some similarities with that of Pa_ASD (identity 42.9%) [17] and Ec_ASD (identity 33.9%) [16]. Although the overall similarities were rather low, amino acid residues belonging to the active site in the ASD enzyme [17] were almost conserved in this protein (Fig. 1). Thus, the ORF was designated as the ASD gene, *asd*. The nucleotide sequence of *asd* from *T. thermophilus* HJ6 was submitted to the DDBJ/EMBL/GenBank nucleotide sequence database under the accession number AFN86158.

3.2. Expression and purification of recombinant Tt_ASD

Recombinant Tt_ASD was expressed in *E. coli* BL21-CodonPlus (DE3) cells (for detail see "Materials and methods") and purified to homogeneity using heat-treatment and metal-chelating chromatography. Sodium dodecyl sulfate-polyacrylamide gel electrophoresis of the purified enzyme yielded one major band, and the molecular mass was determined to be about 37 kDa, which is slightly lower than the molecular mass calculated from the amino acid sequence (38,871 Da) (Fig. 2A). The NH_2-terminal amino acid sequence of the purified recombinant protein was determined to be MDRRRFLV, matching that of the deduced amino acid sequence. The native molecular mass of recombinant Tt_ASD was determined to be about 80 kDa by gel filtration chromatography with a Superdex™ 200 column, indicating that Tt_ASD is a homodimeric enzyme (Fig. 2B).

Reconstitution of the PQQ-bound holoenzyme was carried out as described in the Materials and methods. The ultraviolet–visible (UV) absorption spectra of the unbound apoenzyme and cofactor-bound holoenzyme were measured using a UV-1800 spectrophotometer (Shimadzu).

Upon reconstitution with PQQ, a broad peak corresponding to bound PQQ was observed in the range of 300–400 nm, with a maximum at 342 nm (Fig. 3). The enzyme preparation (1.7 mg/ml, 44.2 μM) showed an absorbance of about 0.40 at 342 nm. Based on a molar absorption coefficient of 9620 $M^{-1}\ cm^{-1}$ at 342 nm [20], the concentration of PQQ-bound enzyme was estimated to be 41.6 μM, which indicates that the fraction of protein molecules bound to PQQ was about 94%.

3.3. Effects of pH and temperature on enzyme activity

To determine the pH-dependence of GDH activity, we employed an overlapping buffer system to cover a pH range of 3.0–9.5. The pH optimum of recombinant Tt_ASD was determined to be 7.0–7.5 (Fig. 4A), lower than that reported for Ec_ASD (optimal pH, 8.75) [16]. The recombinant enzyme showed more than 90% activity within the range of 60–80 °C, and the highest activity was obtained at 70 °C (Fig. 4B). However, valid assays could not be carried out at temperatures above 75 °C due to nonenzymatic decolorization of the dichlorophenol-indophenol test substrate. The holoenzyme was extremely thermostable, retaining full activity after heating for 100 min at 85 °C (Fig. 5), while the apoenzyme hardly retained any activity under the same conditions. Therefore, the heat stability of Tt_ASD was enhanced by reconstitution with PQQ, similar to that previously reported for Pa_ASD [17]. Its high stability at high temperature makes this enzyme potentially useful for applications in biosensors or biofuel cells.

3.4. Substrate specificity

The recombinant Tt_ASD acted upon a broad range of aldose sugars, including hexoses, pentoses, disaccharides, and polysaccharides, in addition to alcohols (Table 1). The sequences of ASDs are conserved and have a common catalytic motif structure (Fig. 1). However, they are diverse in their substrate specificities [16]. The most unusual property of Tt_ASD is that the enzyme can oxidize both ethanol and methanol as substrates, although its catalytic efficiency (k_{cat}/K_m) towards alcohols is much lower than that towards sugars (Table 1). The K_m value for ethanol was much higher than that of the quinoprotein ADHs from *Comamonas testosteroni* (2.23 mM) [21] and *A. calcoaceticus* (0.07 mM) [22]. The catalytic efficiency (k_{cat}/K_m) for ethanol was lower than that of the ADH from *C. testosteroni* (8027 $s^{-1}\ M^{-1}$) [21]. The PQQ-dependent MDHs and type I ADHs have a unique feature; it is necessary to add ammonia, methylamine, or ethylamine as essential activators in standard assays using an artificial electron acceptor such as cationic dyes, PMS, or phenazine ethosulfate [23–26]. It was determined whether

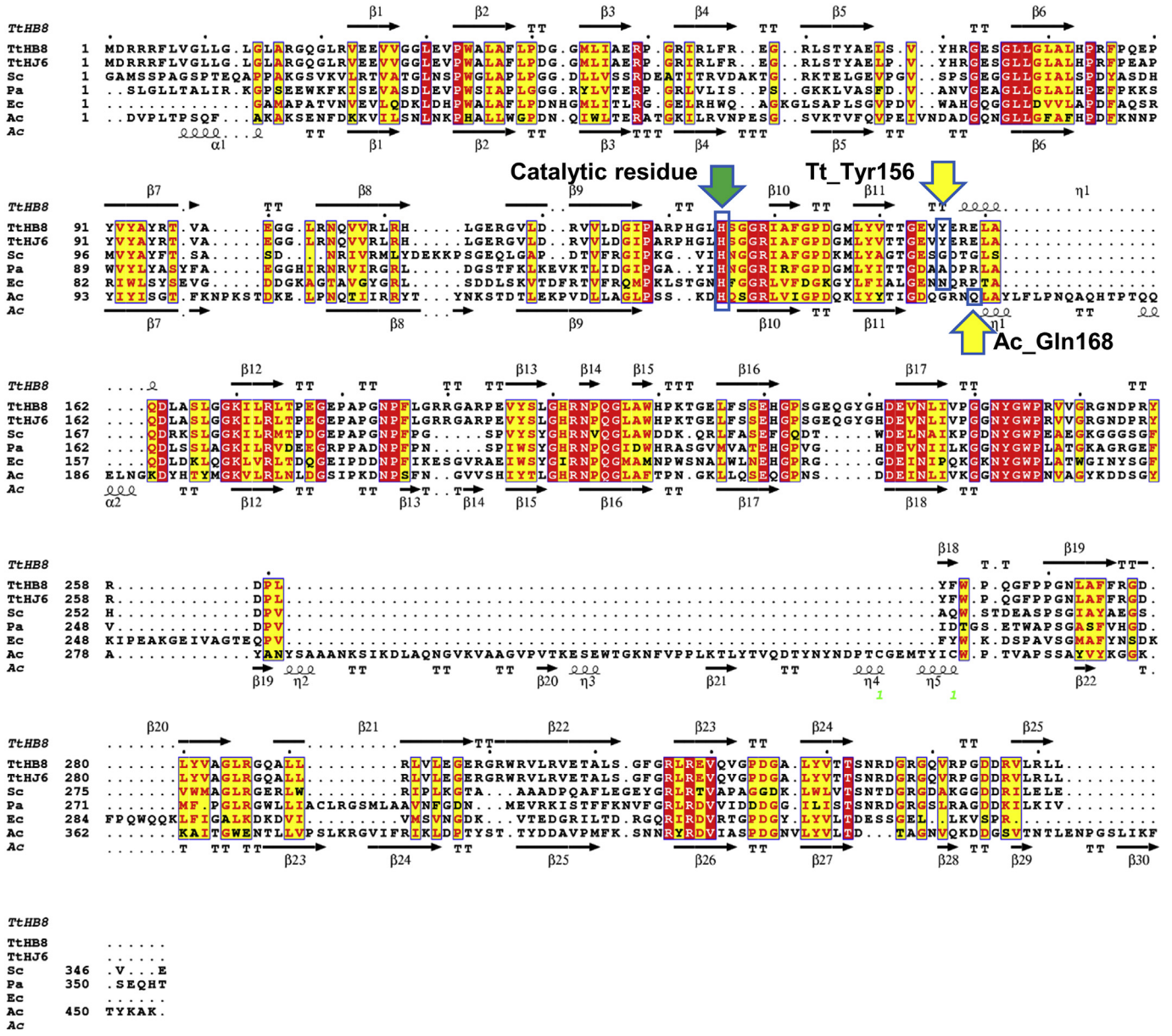

Fig. 1. Alignment of the deduced amino acid sequence of Tt_ASD with its homologues. The sequences were aligned with CLUSTALW and displayed in ESPript along with secondary structure assignments for Tt_ASD (PDB ID: 2ISM) and Ac_ASD (PDB ID: 1CQ1). Strain abbreviation of each protein and Protein ID are as follows: TtHB8, *T. thermophilus* HB8 (UniProtKB code Q5SKS3); TtHJ6, *T. thermophilus* HJ6 (UniProtKB code I7A144); Sc, *Streptomyces coelicolor* (UniProtKB code Q9Z571); Pa, *Pyrobaculum aerophilum* (UniProtKB code Q8ZUN8); Ec, *Escherichia coli* (UniProtKB code M8PTY9); Ac, *Acinetobacter calcoaceticus* (UniProtKB code P13650).

the alcohol dehydrogenase activity of Tt_ASD is activated by NH_4Cl, methylamine, and ethylamine at concentrations between 1 and 100 mM. The ammonia and amines did not affect its alcohol dehydrogenase activity. Therefore, these findings suggest that the catalytic mechanism of Tt_ASD is different from that of the quinoprotein ADH.

Michaelis–Menten type kinetics were observed for the oxidation of D-glucose at 70 °C. The lowest measured K_m value was for glucosamine, the highest k_{cat} value was for α-lactose, and the highest k_{cat}/K_m ratio was for 2-deoxy-glucose. The apparent K_m value for D-glucose was 0.21 M, which is markedly lower than the K_m values obtained with Pa_ASD (0.68 M) and Ec_ASD (0.4 M). In the case of monosaccharides, the enzyme was more specific for D-galactose, D-mannose, L-arabinose, and D-xylose than for D-glucose in terms of its catalytic efficiency, which was reflected by the k_{cat}/K_m ratios. The K_m values of the recombinant enzyme for disaccharides and trisaccharides were lower than those for glucose, leading to a higher catalytic efficiency for all of these substrates than for D-glucose (Table 1). The affinity and catalytic efficiency for all substrates were much higher than those reported for Pa_ASD and slightly lower than those for Ec_ASD.

3.5. Structural and mutational analysis

Three-dimensional (3D) structural analysis can provide a physical basis to understand how Tt_ASD oxidizes alcohols. Tt_ASD is almost identical (only three residues difference) to a putative oxidoreductase (GDH) from *T. thermophilus* HB8, the crystal structure of which has already been determined at 1.9 Å resolution and deposited by the responsible investigators (PDB ID: 2ISM). However, its biochemical properties and structural analysis had not previously been published. This indicates that the deposited model

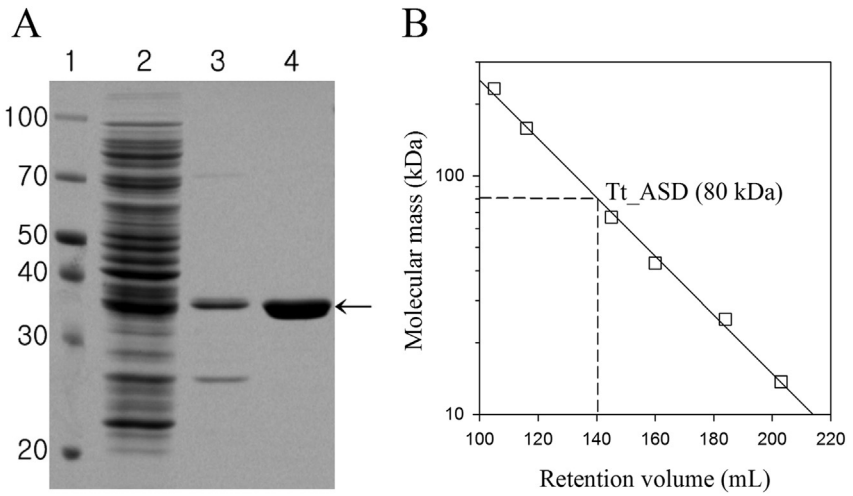

Fig. 2. SDS-PAGE and gel filtration analysis of recombinant Tt_ASD. (A) Purification of recombinant Tt_ASD. M, molecular mass marker; lane 1, crude extract induced cells; lane 2, supernatant of crude extract after heat treatment at 80 °C for 20 min; lane 3, Histrap column peak fractions. The gel was stained with coomassie brilliant blue. (B) Molecular mass determination of recombinant Tt_ASD. The molecular mass of recombinant Tt_ASD was determined by analysis of the elution of standard proteins from a Sephacryl S-200 HR 26/60 column. The column was calibrated with molecular mass standards from GE Healthcare: catalase (232 kDa), aldolase (158 kDa), albumin (67 kDa), ovalbumin (43 kDa), chymotrypsinogen A (25 kDa), ribonuclease A (13.7 kDa).

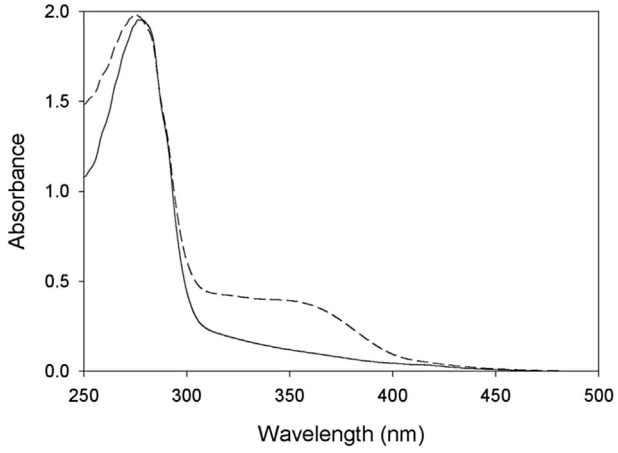

Fig. 3. UV–visible absorption spectra of recombinant Tt_ASD. Absorbance spectra of Tt_ASD before (solid line) and after (dashed line) binding of PQQ.

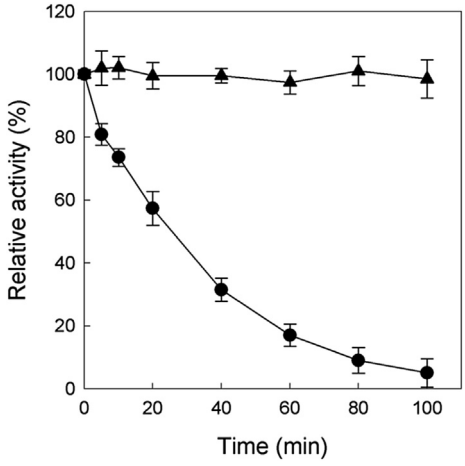

Fig. 5. Thermostability of recombinant Tt_ASD. The apoenzyme (circles) and holoenzyme (triangles) was incubated for various lengths of time at 85 °C, and the residual activity of samples were measured at 70 °C and pH 7.5.

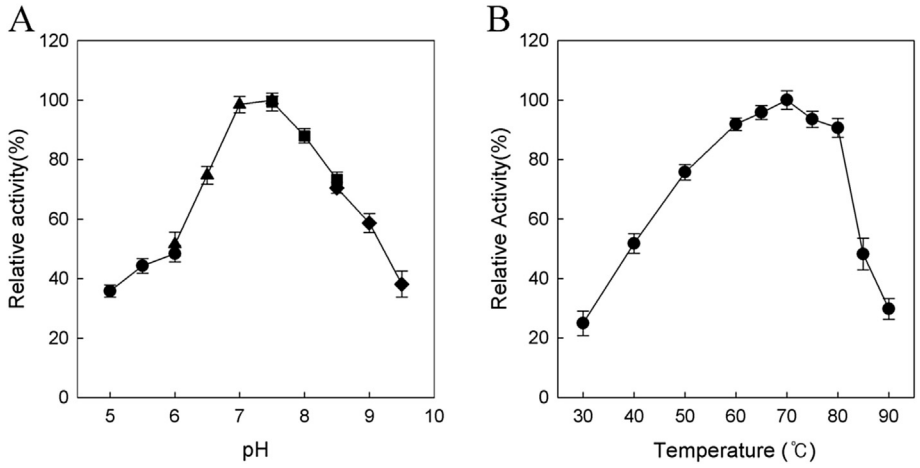

Fig. 4. Effects of pH and temperature on the enzyme activity. (A) pH dependence of the activity. circles, 50 mM sodium acetate; triangles, 50 mM sodium phosphate; squares, 50 mM Tris-HCl; diamonds, 50 mM glycine-NaOH. (B) Temperature dependence of the activity.

Table 1
Kinetic parameters and substrate specificities of the wild type and mutant Tt_ASDs. Data represent the mean (±SE) of duplicate measurements.

Group and name	Wild type			Y156A			Y156K		
	k_{cat} (s^{-1})	K_m (M)	k_{cat}/K_m (s^{-1} M^{-1})	k_{cat} (s^{-1})	K_m (M)	k_{cat}/K_m (s^{-1} M^{-1})	k_{cat} (s^{-1})	K_m (M)	k_{cat}/K_m (s^{-1} M^{-1})
Simple sugars									
D-Glucose	1054 ± 203	0.21 ± 0.08	5021 ± 2543	339 ± 10	0.47 ± 0.03	719 ± 291	316 ± 23	0.25 ± 0.05	1287 ± 485
D-Galactose	823 ± 56	0.11 ± 0.02	7488 ± 2801	160 ± 16	0.38 ± 0.09	417 ± 187	193 ± 6	0.2 ± 0.02	952 ± 333
D-Mannose	1627 ± 311	0.13 ± 0.06	12,518 ± 5199	265 ± 16	0.14 ± 0.03	1858 ± 533	261 ± 18	0.16 ± 0.04	1610 ± 482
L-Arabinose	1755 ± 312	0.16 ± 0.06	10,972 ± 5211	142 ± 10	0.17 ± 0.04	796 ± 264	154 ± 7	0.14 ± 0.02	1079 ± 330
D-Xylose	1681 ± 350	0.14 ± 0.07	12,011 ± 5006	305 ± 46	0.46 ± 0.16	699 ± 291	204 ± 29	0.23 ± 0.10	872 ± 294
D-Ribose	260 ± 103	0.13 ± 0.10	2062 ± 983	181 ± 17	0.07 ± 0.02	2724 ± 835	715 ± 135	0.44 ± 0.13	1631 ± 1034
Alcohols									
Xylitol	15 ± 2	0.09 ± 0.03	173 ± 60	ND[a]	ND	ND	ND	ND	ND
Mannitol	38 ± 4	0.09 ± 0.04	414 ± 103	ND	ND	ND	ND	ND	ND
Methanol	76 ± 42	0.15 ± 0.18	506 ± 237	ND	ND	ND	ND	ND	ND
Ethanol	123 ± 28	0.18 ± 0.10	680 ± 291	ND	ND	ND	ND	ND	ND
Substituted glucose									
2-Deoxy-glucose	1141 ± 162	0.04 ± 0.02	29,483 ± 8503	69 ± 2	0.08 ± 0.01	921 ± 249	128 ± 11	0.14 ± 0.04	903 ± 275
Glucosamine	197 ± 6	0.02 ± 0.00	12,989 ± 2811	104 ± 16	0.02 ± 0.01	5727 ± 1846	117 ± 29	0.02 ± 0.01	8696 ± 2475
Glucose 6-phosphate	192 ± 33	0.08 ± 0.04	2543 ± 918	ND	ND	ND	ND	ND	ND
Disaccharide									
Maltose	1022 ± 150	0.17 ± 0.05	6012 ± 3003	186 ± 20	0.37 ± 0.09	500 ± 222	170 ± 18	0.26 ± 0.07	654 ± 252
α-Lactose	1953 ± 485	0.19 ± 0.09	10,280 ± 5245	282 ± 82	0.64 ± 0.29	439 ± 281	225 ± 61	0.65 ± 0.27	343 ± 221
D-Cellobiose	1042 ± 415	0.07 ± 0.05	14,893 ± 8316	160 ± 17	0.30 ± 0.06	527 ± 280	186 ± 35	0.23 ± 0.05	808 ± 654
Polysaccharide									
Maltotriose	772 ± 247	0.13 ± 0.08	6160 ± 3143	822 ± 169	0.60 ± 0.20	1366 ± 861	363 ± 34	0.16 ± 0.03	2283 ± 961

[a] ND, not detected.

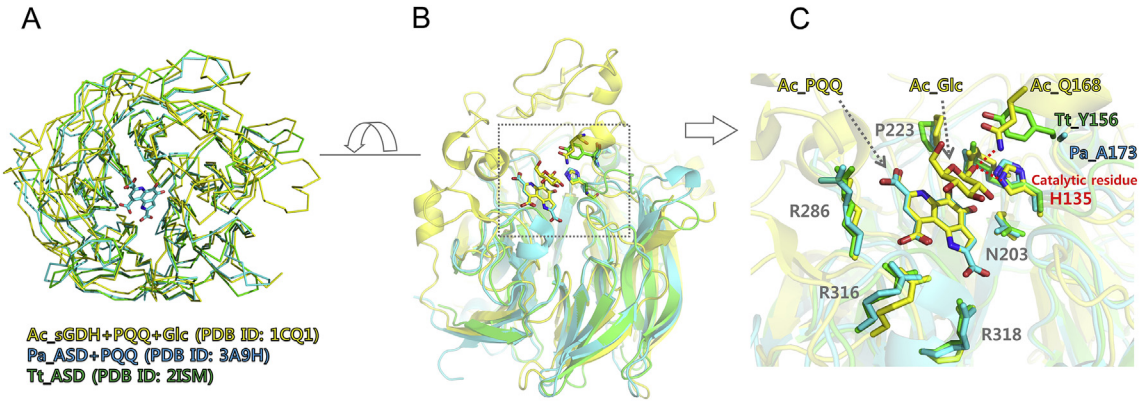

Fig. 6. Structural comparison of three sugar dehydrogenases (Tt_ASD, Pa_ASD and Ac_sGDH). (A) Structural superposition of the three enzymes is represented as ribbon models. (B) The orientation of the cartoon model is rotated 90° around the horizontal axis on the panel A. The open active site is exposed to solvent. The ligand-binding region is indicated as dotted box. (C) Close-up view showing the catalytic and ligand binding site. Residues involved in PQQ and glucose binding are shown as stick models using the same colour code as shown in panel A. The dashed red lines indicate hydrogen bonds. The model structure from the 2ISM PDB entry for putative oxidoreductase from *T. thermophilus* HB8 was regarded as the structure of Tt_ASD. (For interpretation of the references to colour in this figure legend, the reader is referred to the web version of this article.)

structure is identical to the 3D structure of Tt_ASD. Therefore, the deposited structure was regarded as the structure of Tt_ASD in this study. The crystal structure revealed that the overall folding of Tt_ASD consists of the β-propeller folding characteristic of this family containing six four-stranded antiparallel β-sheets. Pa_ASD and Tt_ASD had very similar structures. Comparison of the structure of Tt_ASD with that of Ac_sGDH showed dramatic differences in the structures of the long loop and surface regions (Fig. 6A). The structures of Ac_sGDH complexed with the cofactor PQQ and glucose as substrate and that of Pa_ASD with PQQ were also determined. The three structures of Tt_ASD, Ac_sGDH (PDB ID: 1CQ1), and Pa_ASD (PDB ID: 3A9H) were superimposed by a model of the PQQ molecules fitted by the least-squares approach (Fig. 6A). The catalytic residues and the major residues bound to PQQ were structurally matched with the superimposed structures. In the ligand-complexed structure of Ac_sGDH, the Gln168 residue was found to be involved in hydrogen bonding to glucose as the substrate. The distance between the hydroxyl group of the Tyr156 residue in the structure of Tt_ASD and the hydroxyl O1 group of the glucose molecule in the structure of Ac_sGDH was 4.0 Å in the superimposed structure (Fig. 6C). Gln168 is located within the characteristic long loop of Ac_sGDH, which was found to be significantly shorter in the Tt_ASD structure. The side chain of the Tyr156 residue of Tt_ASD is located in the same structural position as the side chain of the Gln168 residue in Ac_sGDH. The Cα backbone positions of the two proteins were separated by a distance of about 5.1 Å (Fig. 6B and C). This result suggests that Tyr156 might have a substrate-binding role. The results of a multiple sequence alignment showed that Tyr156 is not conserved (Fig. 1). To investigate the role of Tyr156 in the activity of Tt_ASD, two mutants were constructed and enzymatically characterized.

As shown in Table 1, both mutant enzymes showed increased K_m values and decreased k_{cat} values for all of the substrates, indicating that amino acid substitutions of Tyr156 led to impaired activity and

affinity for substrates. The catalytic efficiency of the Y156A mutant was lower than that of the Y156K mutant for most substrates. Furthermore, the Y156A and Y156K mutants lost their activities towards alcohols to an almost undetectable level at a velocity of 1 unit mg^{-1}. These observations confirmed that Tyr156 has a crucial role in determining the substrate affinity and specificity of Tt_ASD. Consequently, these results suggest that the Tyr156 residue plays a unique role in determining the alcohol-binding affinity of Tt_ASD.

4. Conclusion

Taken together, our findings demonstrated that the enzyme Tt_ASD from *T. thermophilus* is highly thermostable in its PQQ-bound holoenzyme form, with activity in the range of 60–80 °C. The enzyme is active at neutral pH (7.0–7.5), and can catalyze the oxidation of various aldose sugars and alcohols. This is the first report of a quinoprotein GDH that shows activity towards alcohols. The information presented in this study contributes to a deeper understanding of sugar metabolism in *T. thermophilus*. Furthermore, these results elucidate the characteristics of an unusual thermostable ASD enzyme with potential applications in the fields of biosensors and biofuel cells.

Conflicts of interest

The authors declare that there are no conflicts of interest regarding the publication of this paper.

Acknowledgement

This work was supported by the Antarctic organisms: Cold-Adaptation Mechanisms and its application grant (PE16070) funded by the Korea Polar Research Institute (KOPRI).

Appendix A. Supplementary data

Supplementary data related to this article can be found at http://dx.doi.org/10.1016/j.abb.2016.08.022.

References

[1] C. Anthony, M. Ghosh, Prog. Biophys. Mol. Biol. 69 (1998) 1–21.
[2] T. Inoue, M. Sunagawa, A. Mori, C. Imai, M. Fukuda, M. Takagi, K. Yano, J. Bacteriol. 171 (1989) 3115–3122.
[3] K. Matsushita, H. Toyami, O. Adachi, Adv. Microb. Physiol. 36 (1994) 247–301.
[4] A.M. Cleton-Jansen, N. Goosen, T.J. Wenzel, P. van de Putte, J. Bacteriol. 170 (1998) 2121–2125.
[5] K. Matsushita, Y. Ohno, E. Shinagawa, O. Adachi, M. Ameyama, Agric. Biol. Chem. 44 (1980) 1505–1512.
[6] S. Igarashi, T. Hirokawa, K. Sode, Biomol. Eng. 21 (2004) 81–89.
[7] S. Igarashi, K. Sode, Mol. Biotechnol. 24 (2003) 97–103.
[8] A. Oubrie, H.J. Rozeboom, K.H. Kalk, J.A. Duine, B.W. Dijkstra, J. Mol. Biol. 289 (1999) 319–333.
[9] A.J. Olsthoorn, T. Otsuki, J.A. Duine, Eur. J. Biochem. 247 (1997) 659–665.
[10] K. Matsushita, E. Shinagawa, O. Adachi, M. Ameyama, Biochemistry 28 (1989) 6276–6280.
[11] A.J. Olsthoorn, J.A. Duine, Arch. Biochem. Biophys. 336 (1996) 42–48.
[12] L. Ye, M. HaÈmmerle, A.J.J. Olsthoorn, W. Schuhmann, H.L. Schmidt, J.A. Duine, A. Heller, Anal. Chem. 65 (1993) 238–241.
[13] G. Gobel, I.W. Schubart, V. Scherbahn, Electrochem. Commun. 13 (2011) 1240–1243.
[14] C. Tanne, G. Gobel, F. Lisdat, Biosens. Bioelectron. 26 (2010) 530–535.
[15] N. Yuhashi, M. Tomiyama, J. Okuda, S. Igarashi, K. Ikebukuro, K. Sode, Biosens. Bioelectron. 20 (2005) 2145–2150.
[16] S.M. Southall, J.J. Doel, D.J. Richardson, A. Oubrie, J. Biol. Chem. 281 (2006) 30650–30659.
[17] H. Sakuraba, K. Yokono, K. Yoneda, A. Watanabe, Y. Asada, T. Satomura, T. Yabutani, J. Motonaka, T. Ohshima, Arch. Biochem. Biophys. 502 (2010) 81–88.
[18] N.Y. Gu, J.L. Kim, H.J. Kim, D.J. You, H.W. Kim, S.J. Jeon, J. Biosci. Bioeng. 107 (2009) 21–26.
[19] F.W. Perrella, Anal. Biochem. 174 (1988) 437–447.
[20] J.A. Duine, J. Frank, J.A. Jongejan, Adv. Enzymol. Relat. Areas Mol. Biol. 59 (1987) 169–212.
[21] A. Geerlof, J.J. Rakels, A.J. Straathof, J.J. Heijnen, J.A. Jongejan, J.A. Duine, Eur. J. Biochem. 226 (1994) 537–546.
[22] J.A. Duine, J. Frank, J. Gen, Microbiology 122 (1981) 201–209.
[23] J.J. Frank, M. Dijkstra, J.A. Duine, C. Balny, Eur. J. Biochem. 174 (1988) 331–338.
[24] M.G. Goodwin, C. Anthony, Biochem. J. 318 (1996) 673–679.
[25] M. Rupp, H. Gorisch, Biol. Chem. Hoppe-Seyler 369 (1988) 431–439.
[26] K. Takeda, T. Ishida, K. Igarashi, M. Samejima, N. Nakamura, H. Ohno, Biosci. Biotechnol. Biochem. 78 (2014) 1195–1198.